Quantitative assessment of forest ecosystem stress caused by cement plant pollution using in situ measurements and sentinel-2 satellite data in a part of the unesco world heritage site

QUANTITATIVE ASSESSMENT OF FOREST ECOSYSTEM STRESS CAUSED BY CEMENT PLANT POLLUTION USING IN SITU MEASUREMENTS AND SENTINEL-2 SATELLITE DATA IN A PART OF THE UNESCO WORLD HERITAGE SITE

ALI ASHARFI[1], YOUSEF ERFANIFARD[1,*], FARSHAD AMIRASLANI[1], ALI DARVISHI BOLOORANI[1], and ALIJAFAR MOUSIVAND[2]

[1] Department of Remote Sensing and GIS, Faculty of Geography, University of Tehran, Tehran, Iran
[2] Department of Remote Sensing and GIS, Tarbiat Modares University, Tehran, Iran
* Corresponding author: erfanifard@ut.ac.ir

ABSTRACT

Anthropogenic industrial dust decreases productivity and slows down the growth of plants. Quantifying the effects of industrial dust on vegetation and determining the distance over which factories scatter dust are of paramount importance for biodiversity conservation and sustaining ecosystem services. This study aims at quantifying the effect of dust emitted by the Neka cement plant (NCP), Mazandaran province, northern Iran, on the surrounding Hyrcanian forests based on an analysis of the Leaf Area Index (LAI) retrieved from Sentinel-2 imagery. An Inductively Coupled Plasma Mass Spectrometer (ICP-MS) was used to quantify the concentrations of cadmium (Cd), chromium (Cr), copper (Cu), lead (Pb), calcium (Ca), magnesium (Mg), sodium (Na), silicon (Si) and zinc (Zn) in leaves of the dominant Chestnut-leaved Oak (*Quercus castaneifolia*). A feed-forward neural network algorithm and field measurements were used to retrieve the leaf area index (LAI) from Sentinel-2 data with a RMSE of 0.42 (m^2/m^2). MODIS-NDVI and EVI time series spanning 17 years (2000 to 2017) were analysed to ensure the independence of the variation in the condition of the vegetation from drought or other environmental factors. The results indicate that Sentinel-2 data can be used to map degradation due to pollution from the cement plant and quantify the effect of the dust spatially. Dust from the cement plant (dust source) was carried approximately 4700 meters in the direction of the prevailing wind. A significant correlation of 0.849 was recorded between LAI and distance from the NCP. It is concluded that dust from the NCP had adverse ecological effects on the neighbouring forest ecosystems recently designated a UNESCO World Heritage Site.

Keywords: BPNN parameter retrival; drought analysis; Hyrcanian forest; industrial dust; leaf area index (LAI); sentinel-2

Introduction

Dust deposited on leaves of plants reduces their ability to photosynthesize and tolerance of drought and other environmental stresses (Shepherd et al. 2016). The adverse effects can be either direct by causing physical and chemical damage to the plants or indirect due to increase in pests and diseases (Manning and Feder 1980). The effect of dust deposition on vegetation depends on the size, accumulation and chemical properties of the dust particles (Yamaguchi et al. 2017). For instance, dust particles larger than stomatal openings (i.e., 8–10 micron) can block stomata and smaller particles may enter into the leaf tissue (Bell et al. 2002). Therefore, dust particles emitted from industrial factories may have significant negative effects on the photosynthesis, growth, and productivity of vegetation.

Dust particles may be of either natural or anthropogenic origin. The manufacture of cement, an anthropogenic source of dust, is the primary source of calcareous particles (Darley 1966). Its manufacture is closely monitored nowadays because of the environmental pollution it causes and also its contribution (approximately 5–7%) to the total anthropogenic emission of CO_2 (Chen et al. 2010). Although different mechanical systems are used to control and collect dust in a cement plant, a considerable amount of dust is still generated and dispersed in the environment during the extraction and crushing of the raw material. Several studies report the emission of major greenhouse gases and atmospheric pollutants, such as CO_2 and SO_2, by the cement industry (e.g. (Capros et al. 2001; Gartner 2004; Josa et al. 2007). Similarly, there are studies of the effects of natural and industrial dust deposition on different types of vegetation based on field measurements (Lal and Ambasht 1982; Prasad and Inamdar 1990; Iqbal and Shafüg 2000; Joshi and Swami 2009; Zia-Khan et al. 2015; Shepherd et al. 2016). Cement dust particles cause a reduction in plant photosynthesis (Darley 1966; Borka 1980; Zia-Khan et al. 2015), plant transpiration (Joshi and Swami 2009) and results in a reduction in chlorophyll content and increase in water loss in plant (Eveling 1969; Chaurasia 2013; Zia-Khan et al. 2015). It is, therefore, critical to quantify accurately the spatial scale over which dust is carried and affects the functioning and productivity of adjacent ecosystems. Among the biochemical and biophysical properties of vegetation that are affected by industrial dust, Leaf Area Index (LAI) is critical in terms of the productivity and ecosystem process of forests and crops at various spatial and temporal scales (Fang et al. 2003). LAI's response to deposition of dust gives a good indication of forest stress (Madejón et al. 2006; Suciu et al. 2008). As a quantitative indicator, LAI indicates the amount of green foliage, photosynthetic capacity and gas-water exchange in an ecosystem (Mousivand 2015). Ground-based measurements of LAI

Asharfi, A., Erfanifard, Y., Amiraslani, F., Boloorani, A. D., Mousivand, A.: Quantitative assessment of forest ecosystem stress caused by cement plant pollution using in situ measurements and Sentinel-2 satellite data in a part of the UNESCO World Heritage Site
European Journal of Environmental Sciences, Vol. 10, No. 1, pp. 22–31
https://doi.org/10.14712/23361964.2020.4

are time-consuming and tedious and often not practical when investigating large areas. Remote sensing, however, provides a faster, non-destructive and an affordable way of estimating LAI at regional to global scales with reliable spatial and temporal resolution (Verstraete et al. 1996; Zheng et al. 2009). Remotely sensed data are frequently used for studying forest biophysical properties and disturbance caused by pests, disease, fire and drought (Entcheva 2000; Frolking et al. 2009; Kennedy et al. 2010; Chen and Meentemeyer 2016; Abdi et al. 2019). There are very few studies assessing the effects of natural and industrial dust on the functioning of vegetation using remote sensing (Toutoubalina and Rees 1999; Persson 2014) and no studies to our knowledge on the use of satellite images to quantify the effects of pollution from cement plants on surrounding forests. There is an increasing interest in understanding and monitoring forests surrounding industrial factories in order to determine the adverse effect of industrial dust on these ecosystems. Because of their widespread distribution and ease of sampling trees are ideal for assessing the effects of pollution (Kardel et al. 2010). However, using conventional ground surveying techniques to do this can be tedious and expensive. Alternatively, remote sensing offers a suitable tool for quantifying and assessing forest stress due to dust deposition.

Hyrcanian forests are a remnant of old-growth forest dating back more than 25 million years. The forests stretch almost 850 km along the northern slopes of the Alborz Mountains on the southern coast of the Caspian Sea and have a rich faunal and floral biodiversity. The critical role of Hyrcanian forests as a valuable native habitat of more than 3,200 species of vascular plants and 240 species of animals recently resulted in registration of these forests as a UNESCO World Heritage Site (July 2019). The Neka cement plant (NCP) is located at the northern edge of the Hyrcanian mixed forests in northern Iran. Field surveys and Visual interpretation of satellite imagery along with public reports indicate that this industry has had an adverse effect on these forests (e.g. https://financialtribune.com). Nevertheless, the adverse effects of dust deposition on the surrounding forest have not yet been studied.

Therefore, the current study uses remotely sensed data to assess the adverse effects of NCP on the neighbouring Hyrcanian forests in northern Iran. The main objective of this study is to evaluate the potential of Sentinel-2 satellite imagery for estimating LAI of forest stands adjacent to the NCP. This study provides information about the reliability of remote sensing technologies for assessing the stress caused by dust emitted during the manufacture of cement to forests and for efficient decision-making for close-to-nature forest management.

Material and Methods

Study area

The Hyrcanian forests on the south side of the Caspian Sea, cover 500 km^2 along 850 km of the mountains from southeast Azerbaijan to the province of Golestan in Iran. These forests have existed here for 25 to 50 million years. Refugia for broad-leaf forests, which was the dominant species in the North Temperate Zone 25-50 million years ago in the early Cenozoic era, existed in this area (Ramezaniet al. 2008). The area studied is located 36.60 to 36.66 N and 53.36 to 53.52 E, in the east of Mazandaran province, at the northern edge of the Hyrcanian mixed forests near the southern shore of the Caspian Sea in Iran. This area includes the NCP, which was established in 1981 (Fig. 1). The minimum, maximum, and average altitudes in the study area are 80, 600 and 300 meters above sea level, respectively. The climate is semi-Mediterranean characterized by mild and humid winters and hot and humid summers. The dominant species of trees in this region are Chestnut-leaved oak (*Quercus castaneifolia*) (hereafter oak), Persian ironwood (*Parrotia persica*), hornbeam (*Carpinus betulus*) and Siberian elm (*Zelkova carpinifolia*). In addition, trees such as maple (*Acer* sp.) and alder (*Alnus* sp.), among others, grow in the valleys and along the rivers. The NCP covers an area of 67 ha. Some of the dust comes from vehicles transporting raw and depositing waste materials, while the rest is emitted from the chimneys of the cement factory. Two chimneys are used for cooling, four are associated with the cement mill and three others with the milling of materials.

Field measurements

To adequately model the accumulation of industrial dust and its effect on vegetation, it is essential to measure the concentration of dust particles and their mineralogical-chemical composition along with plant biophysical properties. To do so, we have quantified the heavy metals on tree leaves by collecting samples and analysing them using an Inductively Coupled Plasma Mass Spectrometer (ICP-MS). Moreover, *in situ,* LAIs were measured to quantitatively estimate the available total area of leaves per unit ground area. Field measurements were made from 17 to 20 September 2017, which corresponds to the vigorous growth period of deciduous trees in the area studied. Leaf samples were collected at 2–3 m above the ground in the four cardinal directions (i.e., north, south, east and west) from the canopies of the trees used for the ICP-MS measurements, with minimum contact with the surface of the leaves.

ICP-MS data

ICP-MS was used to quantify concentrations of cadmium (Cd), chromium (Cr), copper (Cu), lead (Pb), calcium (Ca), magnesium (Mg), sodium (Na), silicon (Si) and zinc (Zn) in leaves of the dominant oak trees. ICP-MS is a powerful tool for tracing many elements and their isotopes with high sensitivity and reliable precision (Bulska and Wagner 2016). The area was divided into 20 squares plots of 250 × 250 m and categorized into different classes according to vegetation and distance

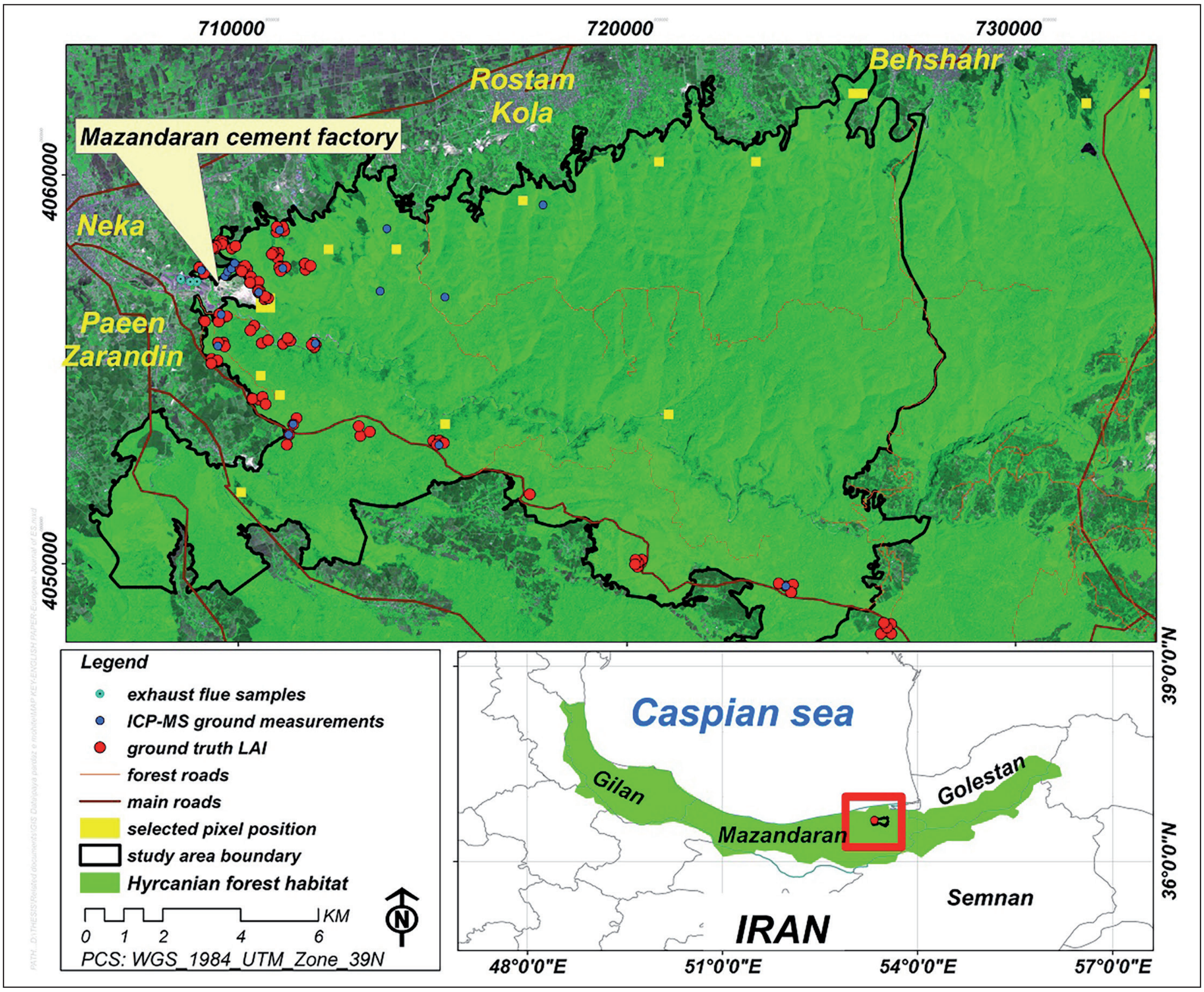

Fig. 1 Map showing locations where ICP-MS samples (blue dots), ground measurements of LAI (red dots), exhaust flue samples (cyan coloured dots) were collected and selected similar pixels (yellow polygons), Hyrcanian forests recently designated a UNESCO World Heritage Site is located along the south coast of the Caspian Sea (light green), study area (rectangular red box) are presented on a true-colour composite (RGB) of Sentinel-2B.

from the NCP (Fig. 1). The detached leaves were stored in labelled plastic bags in a cooling package and transferred to the laboratory. In the laboratory, the leaves were placed in beakers, covered with watch glasses and dried for 48 hours in an oven at 70 °C. Later, these samples were ground and then digested in a closed system using ultra-pure nitric acid and hydrogen peroxide in a microwave oven. ICP-MS multi-element standard solutions were used to determine the concentrations of different heavy metals, which ranged from 0.1 ppb to 100 ppm.

LAI field measurements

Hemispherical (fisheye) photography was used to estimate forest LAI. This technique has been widely and successfully used for estimating the LAI and canopy structures of plants over the past decades (Macfarlane et al. 2000; Chen et al. 2006; Demarez et al. 2008; Wang et al. 2018). Hemispherical images record the spectral and spatial characteristics of the forest canopy, from which direct and scattered light regimes can be estimated (Frazer et al. 2001). A Canon EOS 6D camera, equipped with the Canon lens EF 8–18 mm f/4L, and a spider tripod, equipped with a lever, were used for hemispherical photography. The images were processed by the Gap Light Analyser (GLA) software and used to estimate LAI (Frazer et al. 1999; Olivas et al. 2013; Sadeghi et al. 2016; Fournier and Hall 2017). The GLA is acknowledged to be good and reliable way of estimating LAI.

The measurements were made under a uniformly overcast sky or a clear sky within 2 hours of sunset or sunrise (Breda 2003). To select representative samples, the area studied was divided into several zones based on the distance from the dust source, and random sampling was used in each zone. Measurements were made in the field in four cardinal directions from the NCP as the dust source. A total of 105 measurements were collected from an area of about 30 × 15 km around the factory (Fig. 1). The LAI measurements ranged between 0.94 and 4.5 with a mean of 2.85 and a standard deviation of 1.17.

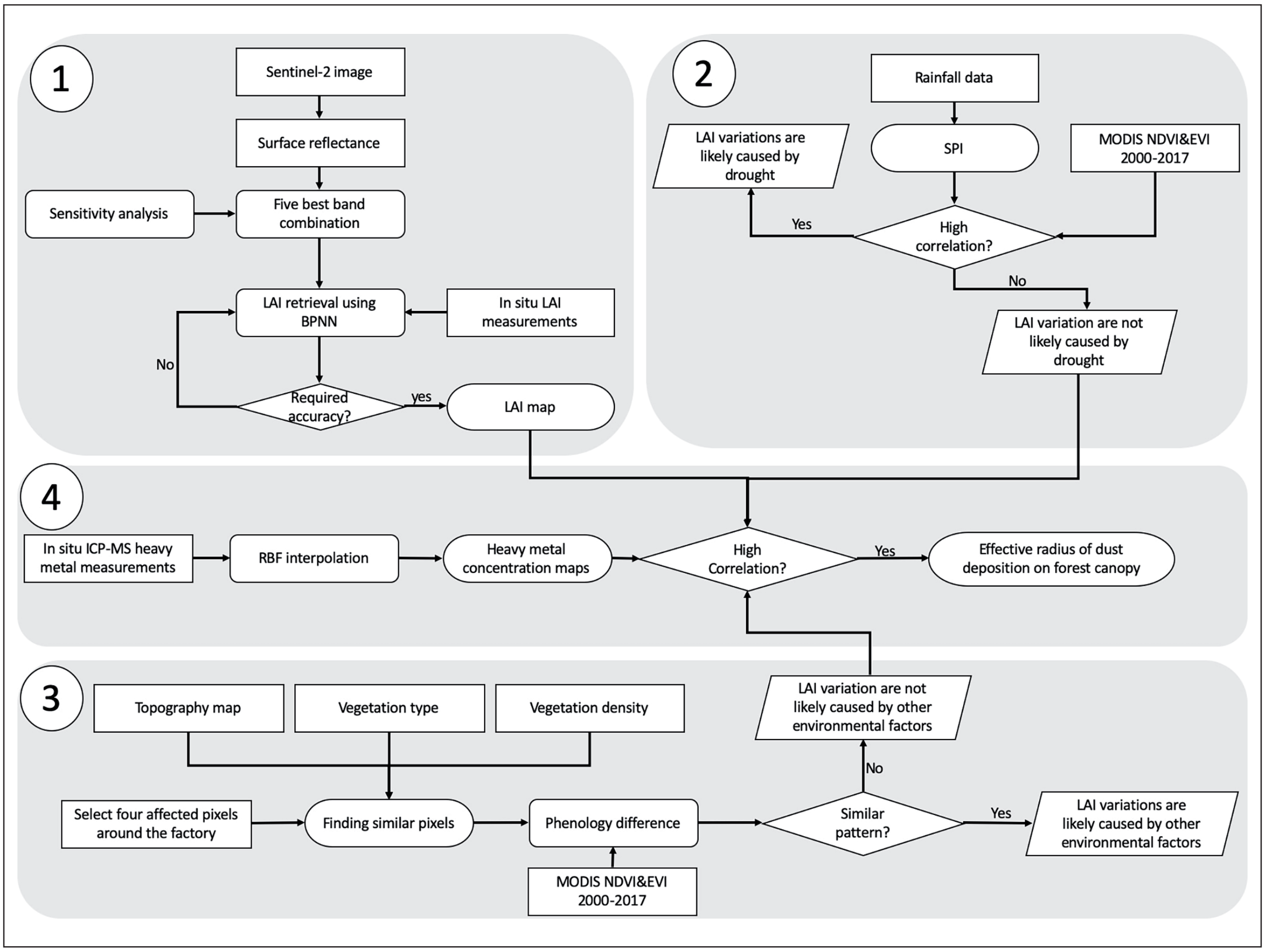

Fig. 2 Flowchart of the methodology. LAI retrieval from Sentinel-2 image of September 22, 2017 (1); was used to check whether variations in LAI were caused by drought (2); or other environmental factors (3); which determine the effective radius of the deposition of dust on the canopy of the forest (4).

Methods

As the main objective of this study was to quantify the effect of dust emitted by NCP on surrounding forests, we first investigated, whether there was any relationship between the deposition of dust particles and health of vegetation in polluted areas based on variation in LAI. We then determined, whether the variation in LAI was the result of contamination with dust, drought or other environmental factors. Finally, the effective radius of dust deposition impact was determined. This analysis required spatially continuous maps of LAI and dust contamination in the area studied. The flowchart of the methods used in this study is given in Fig. 2.

A three-layer Back Propagation Neural Network (BPNN) with one input layer, ten hidden layers and one output layer was used to retrieve LAI from Sentinel-2 satellite images (Foody and Atkinson 2002; Fang et al. 2003). The hyperbolic tangent sigmoid was chosen as the transfer function between the input and hidden layers. The combination of tangent and linear functions is adequate for fitting different kinds of functions for retrieving LAI (Combal et al. 2003; Verger et al. 2011). The satellite image was converted to surface reflectance using the "Sen2Cor" plugin, embedded in SNAP software to remove unwanted atmospheric influences on the recorded signals. Sentinel-2 spectral bands with spatial resolutions of 10 m and 20 m were used where the ten m-spatial resolution bands were resampled into 20 m spatial resolution bands. A sensitivity analysis was used to determine the Sentinel-2 spectral bands most sensitive to LAI (see Mousivand et al. 2014). Trial and error analysis were carried out to determine the most efficient combination of bands for LAI retrieval. Consequently, the five spectral bands most sensitive to LAI were selected for further retrieval. The LAI field measurements were split into 70% training and 30% validation data. For training the BPNN, 10-fold cross-validation was used, in which the training data were divided into ten subsamples. For each, nine subsamples were used to train the model and the remaining subsample as a test set. The final model validation was computed using the independent validation dataset (i.e., 30%). To ensure that the variation in LAI within the area studied was not caused by drought, a drought analysis was done. Firstly, the Standardized Precipitation Index (SPI)

(1-, 2-, 3-, 6- and 12-month SPI) was computed using rainfall data obtained from the meteorological station closest to the dust source for the period 2000-2017. This index is widely used to characterize drought over a range of timescales (e.g., Guttman 1998; Łabędzki 2007). In addition, the relationships between SPI and the different vegetation indices, such as NDVI and EVI, extracted from the MODIS data, were determined for the period 2000-2017. Monthly NDVIs and EVIs were retrieved from 16-day NDVI and EVI MODIS products and their correlations with SPIs were determined for the period of 2000-2017. A close relationship between NDVI and SPI is used as an indicator for determining drought severity and duration of the cover of vegetation (Ji and Peters 2003).

In addition, time series of NDVIs and EVIs were analysed for pixels with similar conditions to ensure that the variations in LAI are not affected by other environmental factors. First, four MODIS pixels around the dust source that were affected by deposition of dust were selected manually. Then, an algorithm was used to find the pixels that share similar characteristics (such as average altitude, slope, aspect, type of vegetation and density) in the east and south directions around the factory. The NDVI and EVI time series were used to interpret phenological differences between contaminated pixels and similar uncontaminated ones and determine if the variations in LAI are due to dust deposition.

Radial basis function (RBF) interpolation was used to generate a map of the area contaminated with heavy metals. This algorithm can be effectively used for interpolation of scattered measurements regardless of the dimensions (Fornberg and Flyer 2005). The interpolated maps provide a graphical representation of spatial variability in the deposition of heavy metals within the area studied. This indicates where the concentration of a specific heavy metal is high and at least where there is a deposition of dust on tree leaves. Finally, the correlation between LAI and deposition of dust was calculated and the spatial scale, at which dust from the NCP has affected the canopy of the forest. Three statistical metrics were used for evaluating the performance of the estimations, including Root Mean Square Error (RMSE), coefficient of determination (R^2) and Mean Absolute Error (MAE).

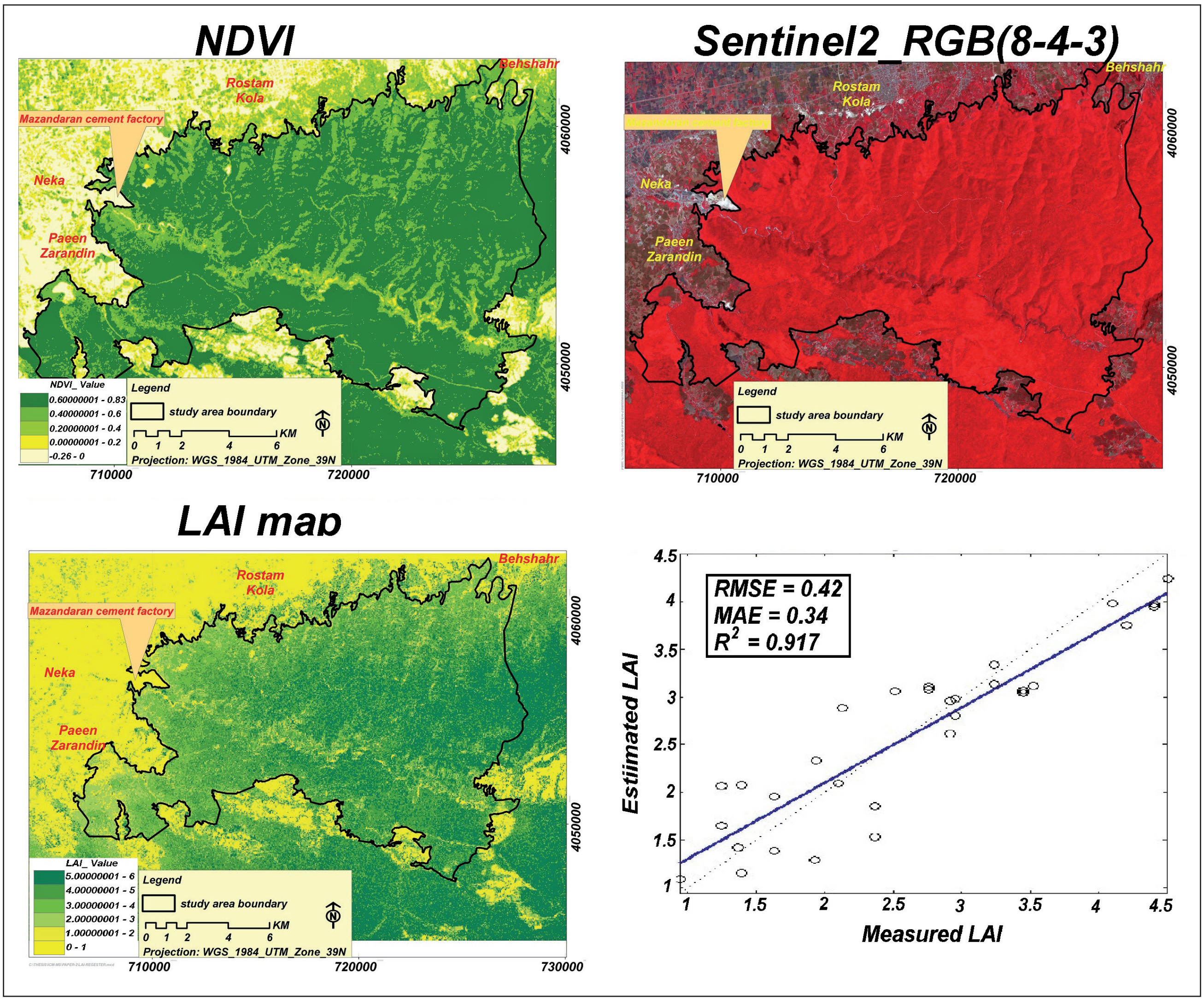

Fig. 3 Estimates of LAI based on Sentinel-2B imagery, NDVI and Sentinel-2B RGB imagery.

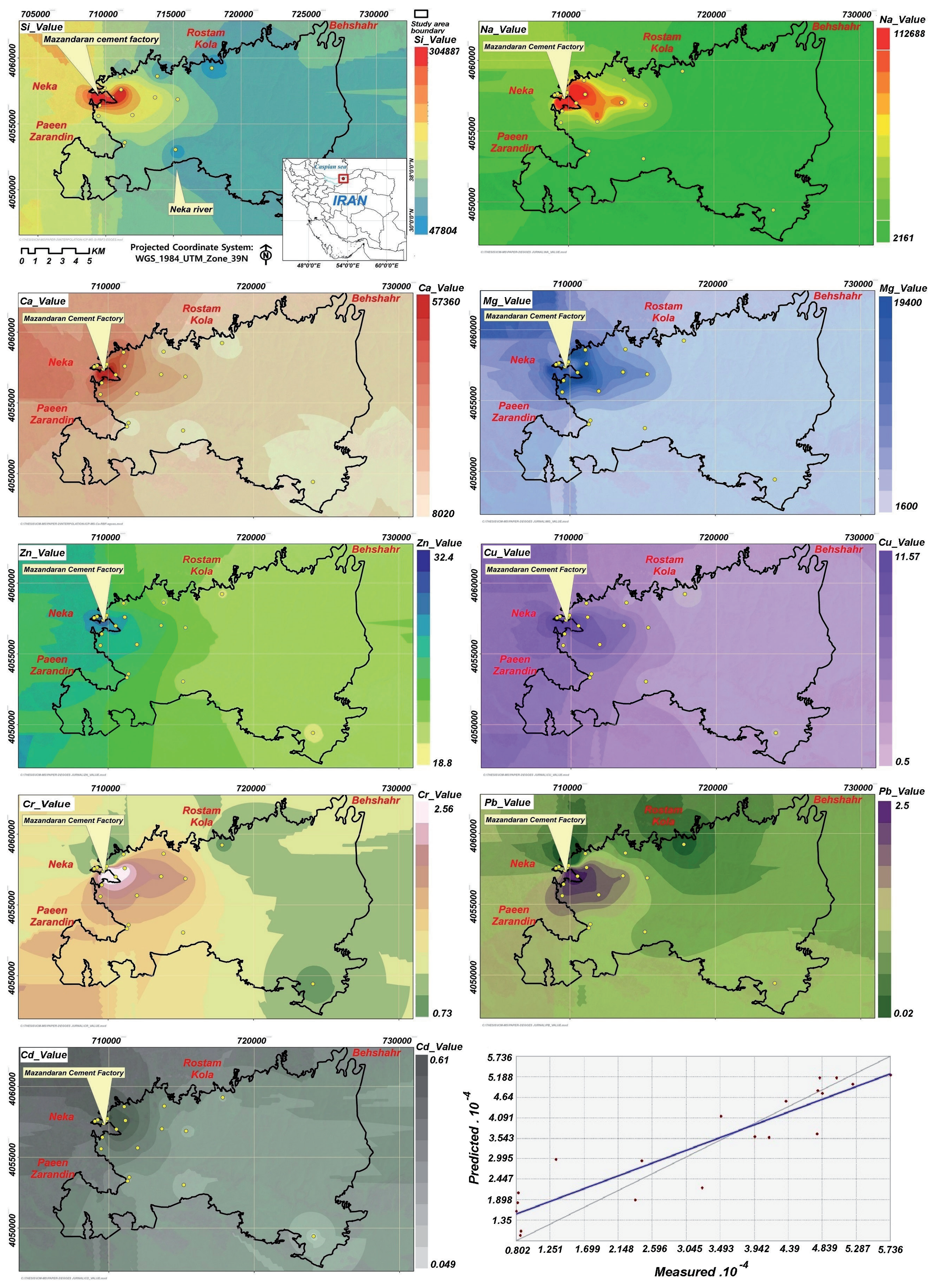

Fig. 4 The spatial distribution of the concentrations of nine heavy metals: cadmium (Cd), chromium (Cr), copper (Cu), lead (Pb), calcium (Ca), magnesium (Mg), sodium (Na), silicon (Si) and zinc (Zn), in leaves of oak trees. Lower right: validation of interpolated results for Ca using the RBF method.

Fig. 5 Examples of deposition of dust on the leaves of oak (Right) and Persian ironwood (Left) growing close to the Neka cement plant.

Results and Discussion

LAI estimation

Accurate estimates of LAI based on satellite data is a prerequisite for quantifying the effects of the deposition of industrial dust on plant health and productivity. To check the performance of the retrieval algorithm, estimates of LAI were validated using an independent dataset consisting of 30% of *in situ* measurements of LAI. The estimate of LAI using RMSE was 0.42 (m^2/m^2) and from MAE based on Sentinel-2 imagery it was 0.34 (m^2/m^2) (Fig. 3). The high value of the coefficient of determination ($R^2 = 0.917$) and low values of RMSE indicated that the linear relationship between the estimated and measured LAI values was strong. In general, a good agreement was found between the predicted and field measurements of LAI, with no systematic discrepancies. These results revealed no major over- or underestimation and, therefore, the retrieval model provided a reliable estimate of LAI. This is in line with results presented in previous studies (e.g., Delegido et al. 2011; Majasalmi et al. 2016; Bochenek et al. 2017; Clevers et al. 2017; Zhang et al. 2017), which report strong relationships between field estimates of LAI and those based on Sentinel-2. This is partly due to the Sentinel-2 red-edge spectral bands for biophysical parameter retrieval (Delegido et al. 2013).

Fig. 3 shows the LAI map derived from Sentinel-2 imagery. The map displays LAIs ranging from 0 (light yellow) to more than 6 (dark green) for areas covered with a wide range of crops and different forest trees. While the lowest LAI was recorded for bare soil, built-up areas and water bodies, the maximum LAI was recorded for closed-canopy forests with nearly complete interception of solar radiation. The NDVI and original Sentinel-2 RGB image are also provided for the sake of comparison and visual interpretation. The estimates of LAI were based on the types of land cover depicted in Fig. 1 and changes in cover of vegetation depicted in the NDVI map.

Spatial distribution of heavy metals

The spatial distribution of nine heavy metals: Cd, Cr, Cu, Pb, Ca, Mg, Na, Si and Zn, are shown in Fig. 4. These maps provide a graphical representation of the spatial variability in the deposition of heavy metals within the area studied and indicate where the concentration of specific heavy metal is highest (or lowest). These maps were generated using RBF spatial interpolation of measurements of heavy metal accumulation in the leaves of oak trees. The RBF interpolation model was compared with other conventional methods such as Inverse Distance Weighted (IDW), Kriging and cubic spline interpolation. Results indicate the RBF method is accurate for almost all heavy metals. Fig. 4 provides an example of a cross-validation for interpolating Ca using the RBF method. The NRMSE value (0.14 for Ca) was the lowest compared with values obtained using other methods. The concentration ranges (all data in mg/kg d.m.) of the different heavy metals were: Cd (0.049–0.61), Cr (0.731–2.56), Cu (0.5–11.57), Pb (0.02–2.455), Zn (18.823–32.357), Ca (8000–57000), Mg (1600–19400), Na (2150–113000) and Si (48000–305000). The spatial distribution of heavy metals was clearly greatly affected by topography and distance from NCP.

The highest accumulation of heavy metals was recorded close to the factory and then decreased with distance from the factory. Similar patterns in the distribution of heavy metals and hazardous gases produced during the manufacture of cement are reported by Zhang et al. (2015) and Atamaleki et al. (2015). However, there was a tendency for the effect to be more significant in the east (Fig. 4) and in the immediate surrounding of the cement factory, which is a major heavy metal concentration hotspot. Large and heavy dust particles are mainly deposited close to the source. Therefore, the accumulation of dust was greatest close to the source. Two examples of leaves collected close to the factory are shown in Fig. 5.

It is noteworthy that oak leaves are rich in Ca, Mg, Na and Si, which is why the recorded concentration of these elements was so high. However, there are no similar studies on the natural concentration of heavy metals in the leaves of trees in the area studied for comparison, however, the average concentrations of Zn, Cr, Cu, Pb and Cd in oak leaves collected from trees located east and south were higher than in those collected from trees located southwest of the cement plant.

Correlation between LAI and dust deposition

The maps depicted in Fig. 4 indicate high concentrations of the heavy metals around the NCP, which decrease with increase in distance from the dust source. However, to obtain a better picture of the effects of the deposition of dust, variations in the vegetation associated with the deposition of dust was measured quantitatively.

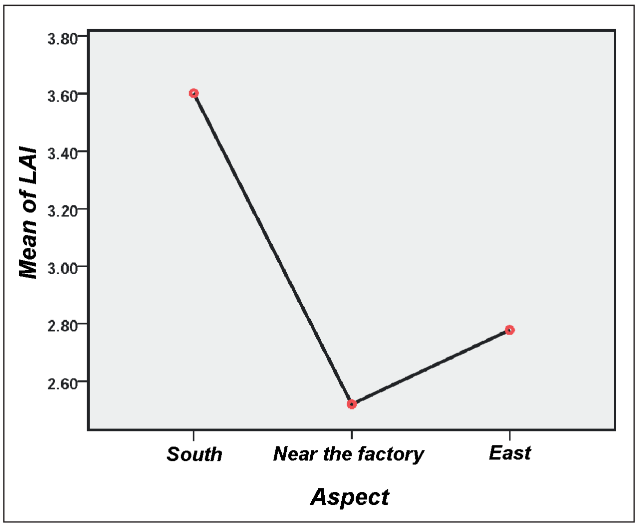

Fig. 6 Average LAI of similar pixels in the south, east and near the Neka cement plant.

Although the plot of the variation in LAI with distance from the factory in different directions quantifies the effect in homogenous areas, it does not accurately quantify the stress in the area studied where the topography and vegetation is very complex. The analysis, therefore, was restricted to a limited number of similar minute areas. Some of the areas around the factory were identified as affected during the field survey. Other minute areas that were similar in terms of slope, aspect and type and density of vegetation, allowing for a variation of up to 5% in in the different factors, were also selected. A total of 3125 similar areas were identified in the area studied.

North and west of NCP was agricultural land, which was not included in this study, the analysis only included areas in the south, east and close to NCP. A distance of 500 m around the factory was considered to be close to NCP. Based on the heavy metal contamination recorded during the field survey three regions were characterized with average LAIs of 2.55, 2.80 and 3.63 close to, east and south of NCP, respectively (Fig. 6). Since similar pixels in terms of LAI, were carefully selected the lowest LAI close to the NCP and to the east of NCP are likely to be linked to a significant effect of the dust on forest LAI. A significant effect was recorded close to the NCP, where a difference of 1.08 was recorded compared to less affected LAIs in the south. These results are in good agreement with the concentration maps, which indicates that the dust particles are mainly carried by the prevailing wind. Although average LAI reflects the overall effect of dust, it does not provide information on the distribution and extent of the variation. Therefore, measures of dispersion including variance, skewness and kurtosis were also considered and normality of the data tested. From the results of the p-p plot test, skewness, and kurtosis values, it is concluded that LAI values are normally distributed. Furthermore, a statistical hypothesis test was used to assess the statistical significance of the difference between the properties (average and variance) of LAI in different areas. The results of hypothesis tests revealed a significant relationship between LAI and the direction from the factory with a confidence level of 5%. Moreover, a significant correlation (0.849) was recorded between LAI (dependent variable) and distance from the NCP (independent variable). This relationship increased for the pixels within 4700 meters of the source of the pollution, after which they ceased increasing and became almost stable. Likewise, a strong correlation was found between Cr, Cu, Cd, Pb, Mg, and Na concentrations and distance from the factory with a similar increase up to 4700 m. However, concentrations of Zn, Ca and Si did not show consistent increase with distance. We therefore conclude that this distance is the spatial scale over which dust particles cause meaningful changes in LAI and reduce functioning of the vegetation.

Analysis of possible effects of drought

In addition, the correlations between NDVIs and EVIs, and SPIs were assessed to ensure that the variations in LAI were not caused by drought or other environmental stresses. The relationship between NDVI/EVI and SPI within the area studied was low (<0.2) with lags of up to 12 months, which indicates there is no evidence of drought. Therefore, it was concluded that the variations in LAI in the area studied was not due to drought. In addition, the 17 year time series of NDVI and EVI were compared to check whether the changes in LAI were due to local anomalies or other local stresses, but no evidence was found to support such a claim.

Conclusions

The main aim of this study was to quantify the response of the Hyrcanian mixed forest to stress caused by industrial dust produced during the manufacture of cement. To do so, ground-based measurements of LAI, chlorophyll, and spectroscopy were made concurrently with the satellite observations. Moreover, leaf samples were collected to measure the concentration of nine heavy metals using ICP-MS. A MODIS-LAI time series was used to test whether the stress was caused by drought or other environmental factors.

The significant finding of this study was that the adverse effect of industrial dust deposition on the leaves of the trees in the surrounding forest could be quantitatively mapped using the LAI extracted from Sentinel-2 satellite data. To the best of our knowledge, there is no study on the quantification of the effect of industrial dust using satellite data. We also recorded strong relationships between ground measurements of LAI and those obtained using Sentinel-2 data. The results are promising because the relationship between the variation in LAI and distance from the dust source, i.e., NCP, was strong and associated with heavy metal concentrations. We found that the dust produced by the cement plant caused an average decrease in LAI of 1.08 in the immediate surroundings of the factory and 0.83 in the easterly direction In contrast, south of the factory was less affected. This highlighted the role of prevailing wind and topography in spreading dust and dust deposition. In this study, we quantitatively mapped the dust deposition over a distance of 4700 m both east and south of the factory. This study revealed that the dust reduced the growth of oak trees and caused them to shed their leaves, which is likely to account for the low LAI values recorded. Drought analysis using the time series SPI and NDVI/EVI revealed no clear evidence for the variations in LAI being due to drought or other environmental factors. Consequently, the variation in LAI is inferred to be due to the direct effect of the dust produced during the manufacture of cement.

Based on this study, changes in forests due to dust deposition can be closely monitored using remote sensing. This study provides evidence that dust from industrial processes, specifically cement manufacture, is deposited on the surrounding environment. The results further our understanding of the interaction between a forest ecosystem and deposition of industrial dust produced by the manufacture of cement and reveal that the new generation of multispectral satellite data, such as Sentinel-2, can be used to detect the effect of pollution on forests.

REFERENCES

Abdi O (2019) Climate–Triggered Insect Defoliators and Forest Fires Using Multitemporal Landsat and TerraClimate Data in NE Iran: An Application of GEOBIA TreeNet and Panel Data Analysis. Sensors 19: 3965, https://doi.org/10.3390/s19183965.

Atamaleki A, Zarandi S M, Fakhri Y, Mehrizi E A, Hesam G, Faramarzi M, Darbandi M (2019) Estimation of air pollutants emission (PM10, CO, SO_2, and NO_x) during development of the industry using AUSTAL 2000 model: A new method for sustainable development, MethodsX 6: 1581–1590, https://doi.org/10.1016/j.mex.2019.06.010.

Bell JN, Bell N, Treshow M (eds) (2002) Air pollution and plant life. John Wiley and Sons.

Bochenek Z, Dąbrowska-Zielińska K, Gurdak R, Niro F, Bartold M, Grzybowski P (2017) Validation of the LAI biophysical product derived from Sentinel-2 and Proba-V images for winter wheat in western Poland. Geoinf Issues 9: 15–26.

Borka G (1980) The effects of cement dust pollution on growth and metabolism of Helianthus annuus. Environ Pollut 22: 75–79.

Breda NJJ (2003) Ground-based measurements of leaf area index: a review of methods, instruments, and current controversies. J Exp Bot 54: 2403–2417, https://doi.org/10.1093/jxb/erg263.

Bulska E, Wagner B (2016) Quantitative aspects of inductively coupled plasma mass spectrometry. Philos Trans R Soc A Math Phys Eng Sci 374:20150369, https://doi.org/10.1098/rsta.2015.0369.

Capros P, Kouvaritakis N, Mantzos L (2001) Economic Evaluation of Sectoral Emission Reduction Objectives for Climate Change. Top-down Analysis of Greenhouse Gas Emission Reduction. European Commission.

Chaurasia S (2013) Effect of cement industry pollution on chlorophyll content of some crops at Kodinar, Gujarat, India. Proc Int Acad Ecol Environ Sci 3: 288–295.

Chen C, Habert G, Bouzidi Y, Jullien A (2010) Environmental impact of cement production: detail of the different processes and cement plant variability evaluation. J Clean Prod 18: 478–485.

Chen G, Meentemeyer RK (2016) Remote sensing of forest damage by diseases and insects. In: Remote Sens Sustain, Weng Q (eds) CRC Press, Taylor and Francis Group, Boca Raton, Florida, pp 145–162.

Chen JM, Govind A, Sonnentag O, Zhang Y, Barr A, Amiro B (2006) Leaf area index measurements at Fluxnet-Canada forest sites. Agric For Meteorol 140: 257–268.

Clevers J, Kooistra L, van den Brande M (2017) Using Sentinel-2 Data for Retrieving LAI and Leaf and Canopy Chlorophyll Content of a Potato Crop. Remote Sens 9: 405–420, https://doi.org/10.3390/rs9050405.

Combal B, Baret F, Weiss M, Trubuil A, Macé D, Pragnère A, Myneni R, Knyazikhin Y, Wang L (2003) Retrieval of canopy biophysical variables from bidirectional reflectance using prior information to solve the ill-posed inverse problem. Remote Sens Environ 84: 1–15, https://doi.org/10.1016/S0034-4257(02)00035-4.

Darley EF (1966) Studies on the effect of cement-kiln dust on vegetation. J Air Pollut Control Assoc 16: 145–150, https://doi.org/10.1080/00022470.1966.10468456.

Delegido J, Verrelst J, Meza CM, Rivera J P, Alonso L, Moreno J (2013) A red-edge spectral index for remote sensing estimation of green LAI over agroecosystems. Eur J Agron 46: 42–52, https://doi.org/10.1016/J.EJA.2012.12.001.

Delegido Jesús, Verrelst J, Alonso L, Moreno J (2011) Evaluation of Sentinel-2 Red-Edge Bands for Empirical Estimation of Green LAI and Chlorophyll Content. Sensors 11: 7063–7081, https://doi.org/10.3390/s110707063.

Demarez V, Duthoit S, Baret F, Weiss M, Dedieu G (2008) Estimation of leaf area and clumping indexes of crops with hemispherical photographs. Agric For Meteorol 148: 644–655, https://doi.org/10.1016/j.agrformet.2007.11.015.

Entcheva PK (2000) Remote sensing of forest damage in the Czech Republic using hyperspectral methods. PhD Thesis, New Hampshire University, Durham.

Eveling DW (1969) Effects of spraying plants with suspensions of inert dusts. Ann Appl Biol 64: 139–151, https://doi.org/10.1111/j.1744-7348.1969.tb02864.x.

Fang H, Liang S, Kuusk A (2003) Retrieving leaf area index using a genetic algorithm with a canopy radiative transfer model. Remote Sens Environ 85: 257–270, https://doi.org/10.1016/S0034-4257(03)00005-1.

Foody GM, Atkinson PM (eds) (2002) Uncertainty in remote sensing and GIS, John Wiley and Sons, Hoboken, NJ, https://doi.org/10.1111/j.0031-868X.2004.282_2.x.

Fornberg B, Flyer N (2005) Accuracy of radial basis function interpolation and derivative approximations on 1-D infinite grids. Adv Comput Math 23: 5–20, https://doi.org/10.1007/s10444-004-1812-x.

Fournier RA, Hall RJ (eds)(2017) Hemispherical Photography in Forest Science: Theory, Methods, Applications, Springer, Dordrecht, Netherlands, https://doi.org/10.1007/978-94-024-1098-3.

Frazer GW, Canham CD, Lertzman KP (1999) Gap Light Analyzer (GLA), Version 2.0: Imaging software to extract canopy structure and gap light transmission indices from true-colour fisheye photographs. Simon Fraser University, Burnaby, British Columbia, and the Institute of Ecosystem Studies, Millbrook, New York.

Frazer Gordon W, Fournier RA, Trofymow JA, Hall RJ (2001) A comparison of digital and film fisheye photography for analysis of forest canopy structure and gap light transmission. Agric

For Meteorol 109: 249–263, https://doi.org/10.1016/S0168-1923(01)00274-X.

Frolking S, Palace MW, Clark DB, Chambers JQ, Shugart HH, Hurtt GC (2009) Forest disturbance and recovery: A general review in the context of spaceborne remote sensing of impacts on aboveground biomass and canopy structure. J Geophys Res Biogeosciences 114: 1–27, https://doi.org/10.1029/2008JG000911.

Gartner E (2004) Industrially interesting approaches to "low-CO_2" cements. Cem Concr Res 34: 1489–1498.

Guttman NB (1998) Comparing the palmer drought index and the standardized precipitation index. J Am Water Resour Assoc 34: 113–121, https://doi.org/10.1111/j.1752-1688.1998.tb05964.x.

Iqbal MZ, Shafüg M (2000) Periodical Effect of Cement Dust Pollution on the Growth of Some Plant Species. Turk J Botany 25: 19–24.

Ji L, Peters AJ (2003) Assessing vegetation response to drought in the northern Great Plains using vegetation and drought indices. Remote Sens Environ 87: 85–98.

Josa A, Aguado A, Cardim A, Byars E (2007) Comparative analysis of the life cycle impact assessment of available cement inventories in the EU. Cem Concr Res 37: 781–788.

Joshi PC, Swami A (2009) Air pollution-induced changes in the photosynthetic pigments of selected plant species. J Environ Biol 30: 295–298.

Kardel F, Wuyts K, Babanezhad M, Vitharana UWA, Wuytack T, Potters G, Samson R (2010) Assessing urban habitat quality based on specific leaf area and stomatal characteristics of Plantago lanceolata L. Environ Pollut 158: 788–794, https://doi.org/10.1016/j.envpol.2009.10.006.

Kennedy RE, Yang Z, Cohen WB (2010) Detecting trends in forest disturbance and recovery using yearly Landsat time series: 1. LandTrendr - Temporal segmentation algorithms. Remote Sens Environ 114: 2897–2910.

Łabędzki L (2007) Estimation of local drought frequency in central Poland using the standardized precipitation index SPI. Irrig Drain 56: 67–77, https://doi.org/10.1002/ird.285.

Lal B, Ambasht RSS (1982) Impact of cement dust on the mineral and energy concentration of Psidium guayava. Environ Pollut Ser A Ecol Biol 29: 241–247, https://doi.org/10.1016/0143-1471(82)90065-4.

Macfarlane C, Coote M, White DA, Adams MA (2000) Photographic exposure affects indirect estimation of leaf area in plantations of Eucalyptus globulus Labill. Agric For Meteorol 100: 155–168.

Madejón P, Marañón T, Murillo JM (2006) Biomonitoring of trace elements in the leaves and fruits of wild olive and holm oak trees. Sci Total Environ 355: 187–203.

Majasalmi T, Rautiainen M (2016) The potential of Sentinel-2 data for estimating biophysical variables in a boreal forest: a simulation study. Remote Sens Lett 7: 427–436, https://doi.org/10.1080/2150704X.2016.1149251.

Manning WJ, Feder WA (1980) Biomonitoring air pollutants with plants. Applied Science Publishers London, England.

Mousivand A (2015) Retrieval of vegetation properties using Top of Atmosphere radiometric data A multi-sensor approach. PhD Thesis, Delft University of Technology, The Netherlands.

Mousivand AJ, Menenti M, Gorte B, Verhoef W (2014) Global sensitivity analysis of the spectral radiance of a soil-vegetation system. Remote Sens Environ 145: 131–144, https://doi.org/10.1016/j.rse.2014.01.023.

Olivas PC, Oberbauer SF, Clark DB, Clark DA, Ryan MG, O'Brien JJ, Ordoñez H (2013) Comparison of direct and indirect methods for assessing leaf area index across a tropical rain forest landscape. Agric For Meteorol 177: 110–116, https://doi.org/10.1016/j.agrformet.2013.04.010.

Prasad MSV, Inamdar JA (1990) Effect of cement kiln dust pollution on groundnut (Arachis hypogaea). Indian Bot contactor 7: 159–162.

Persson S (2014) Estimating leaf area index from satellite data in deciduous forests of southern Sweden. Master's Degree, Lund University, Sweden.

Ramezani, E, Marvie Mohadjer MR, Knapp HD, Ahmadi H, Joosten H (2008) The late-Holocene vegetation history of the Central Caspian (Hyrcanian) forests of northern Iran. The Holocene 18: 307–321, https://doi.org/10.1177/0959683607086768.

Sadeghi SMM, Attarod P, Van Stan JT, Pypker TG (2016) The importance of considering rainfall partitioning in afforestation initiatives in semiarid climates: A comparison of common planted tree species in Tehran, Iran. Sci Total Environ 568: 845–855, https://doi.org/10.1016/j.scitotenv.2016.06.048.

Shepherd G, Terradellas E, Baklanov A, Kang U, Sprigg W, Nickovic S, et al. (2016) Global Assessment of Sand and Dust Storms. United Nations Environment Programme, Nairobi.

Suciu I, Cosma C, Todică M, Bolboacă SD, Jäntschi L (2008) Analysis of soil heavy metal pollution and pattern in central Transylvania. Int J Mol Sci 9: 434–453, https://doi.org/10.3390/ijms9040434.

Toutoubalina OV, Rees WG (1999) Remote sensing of industrial impact on Arctic vegetation around Noril'sk, northern Siberia: Preliminary results. Int J Remote Sens 20: 2979–2990, https://doi.org/10.1080/014311699211561.

Verger A, Baret F, Camacho F (2011) Optimal modalities for radiative transfer-neural network estimation of canopy biophysical characteristics: Evaluation over an agricultural area with CHRIS/PROBA observations. Remote Sens Environ 115: 415–426, https://doi.org/10.1016/j.rse.2010.09.012.

Verstraete MM, Pinty B, Myneni RB (1996) Potential and limitations of information extraction on the terrestrial biosphere from satellite remote sensing. Remote Sens Environ 58: 201–214, https://doi.org/10.1016/S0034-4257(96)00069-7.

Wang J, Xiong Q, Lin Q, Huang H (2018) Feasibility of using mobile phone to estimate forest Leaf Area Index: a case study in Yunnan Pine. Remote Sens Lett 9: 180–188, https://doi.org/10.1080/2150704X.2017.1399470.

Yamaguchi T, Watanabe M, Noguchi I, Koike T (2017) Tree Decline at the Somma of Lake Mashu in Northern Japan. In: Takeshi I (ed) Air Pollution Impacts on Plants in East Asia. Springer, Tokyo, pp. 135–150.

Zheng G, Moskal LM (2009) Retrieving Leaf Area Index (LAI) Using Remote Sensing: Theories, Methods, and Sensors. Sensors 9: 2719–2745, https://doi.org/10.3390/s90402719.

Zhang C, Pattey E, Liu J, Cai H, Shang J, Dong T (2017) Retrieving leaf and canopy water content of winter wheat using vegetation water indices. Appl Earth Obs Remote Sens 11: 12–126.

Zhang S, Worrell E, Crijns-Graus W (2015) Cutting air pollution by improving energy efficiency of China's cement industry, energy procedia, Elsevier 83: pp 10–20, https://doi.org/10.1016/j.egypro.2015.12.191.

Zia-Khan S, Spreer W, Pengnian Y, Zhao X, Othmanli H, He X, Müller J (2015) Effect of dust deposition on stomatal conductance and leaf temperature of cotton in Northwest China. Water (Switzerland) 7: 116–131, https://doi.org/10.3390/w7010116.